Power Electronics and Applications (EPE 2018 ECCE Europe), 2018 20th European Conference on

IGCT Switching Behaviour Under Resonant Operating Conditions

D. Stamenkovic, D. Dujic, U. Vemulapati, *et al.*

POWER ELECTRONICS LABORATORY
ÉCOLE POLYTECHNIQUE FÉDÉRALE DE LAUSANNE

IGCT Switching Behaviour Under Resonant Operating Conditions

Dragan Stamenkovic, Drazen Dujic
Power Electronics Laboratory
École Polytechnique Fédérale de Lausanne
Station 11
Lausanne, Switzerland
Email: dragan.stamenkovic@epfl.ch,
drazen.dujic@epfl.ch
URL: http://pel.epfl.ch

Munaf Rahimo, Umamaheswara Reddy
Vemulapati, Thomas Stiasny
ABB Semiconductors
Fabrikstrasse 3
Lenzburg, Switzerland
Email: munaf.rahimo@ch.abb.com,
umamaheswara.vemulapati@ch.abb.com,
thomas.stiasny@ch.abb.com

Acknowledgments

The work presented in the paper is supported in part by the Swiss National Science Foundation under the project number 200021_165566 and in part by ABB Semiconductors, Lenzburg, Switzerland.

Keywords

≪Integrated Gate Controlled Thyristor≫, ≪Resonant Converter≫, ≪Medium Voltage High Power DC-DC converter≫, ≪Solid State Transformer≫

Abstract

In the area of medium voltage DC-DC conversion, LLC Series Resonant Converter (LLC-SRC) presents itself as an attractive topology for implementation of the DC transformer. Employing Integrated Gate-Commutated Thyristor (IGCT) as a switching element one can obtain very low conduction losses with this design, while considerably lowering the switching losses. Low current turn-off of the switch previously flooded with the high quasi sinusoidal load current is explored throughout this paper. Conclusions are supported by Technology Computer Aided Design (TCAD) simulations and by waveforms obtained from a dedicated test setup designed to emulate the conduction and switching conditions present in LLC-SRC.

Introduction

Expanded research interests in MVDC power distribution networks with DC-DC converters acting as a DC transformers yields a motivation of exploring the IGCT technology. Considerable amount of research was already done in the field, mostly based on Insulated Gate Bipolar Transistor (IGBT) technology [1], [2] for its popularity and availability. IGCT technology is found to be an encouraging alternative to IGBT and has already proven itself in the applications such as medium voltage drives [3] and rectifiers [4]. This mature technology has previously found its place in the grid interties, variable speed drives, solid state breakers [5] etc. with over 1GW of installed power in numerous pieces of equipment [3]. Hard switching of the semiconductor device under large currents and switching frequencies up to 900Hz is one common aspect for all of these applications.

Regardless of the IGBT being preferred semiconductor of choice in most of the proposed converter topologies, IGCT as a switching device offers various advantages over IGBT [6]. Given its thyristor structure, conduction losses of the IGCT are significantly lower when compared to the IGBT of the same rating; turn-on losses can usually be neglected (due to inductive load current) while turn-off losses are comparable to that of IGBT. Additional positive aspects are high short circuit capability, high reliability

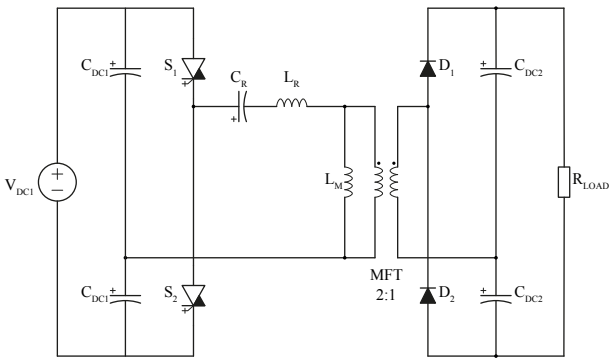

Fig. 1: Half bridge LLC-SRC

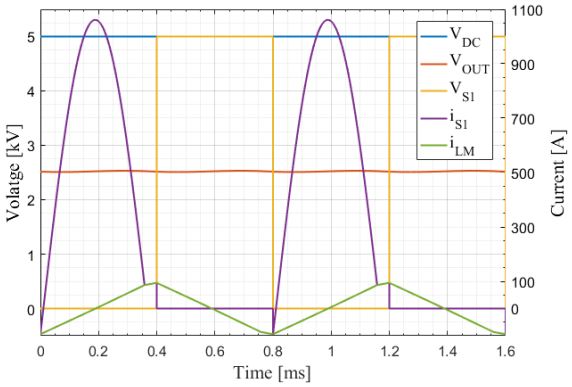

Fig. 2: LLC-SRC characteristic waveforms

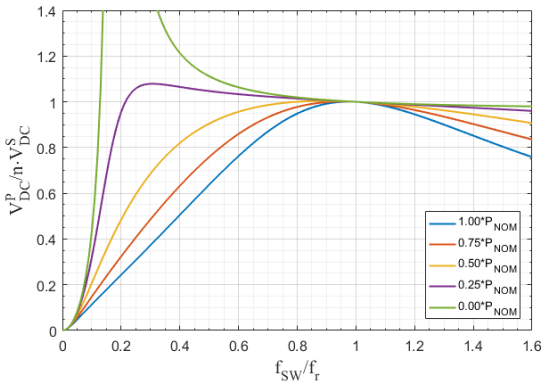

Fig. 3: LLC-SRC transfer characteristic

Table I: LLC-SRC Parameters

Parameter	Value
V_{DC1}	5000V
V_{DC2}	2500V
C_R	80 μF
L_R	167 μH
L_M	5 mH
C_{DC2}	5.64 mF
R_{LOAD}	4.17 Ω
f_{SW}	1250 Hz
f_R	1375 Hz

and large Safe Operating Area (SOA) as well as the better utilization of the silicon surface for the same type of packaging (press-pack) allowing IGCT higher current carrying capability (full circular surface of silicon opposed to number of IGBT rectangular dies on a round surface of a package). Explored unfavorable aspects include relatively large gate driver circuitry and lack of di/dt control during turn-on which introduces the requirement of the clamp circuit for hard switching applications (but helps in limiting the short circuit current), further increasing number of components needed for the final converter circuit.

Application of the IGCT in the resonant converter topologies (e.g. [7]) presents the opportunity to further maximize its performance: low current turn-off could lead to significant decrease in accompanying energy losses, leaving it only with conduction losses which are already the lowest among the similar switching devices. The structure and the role of the clamp circuit in resonant operation should be reconsidered because of the low turn-on di/dt due to the presence of the resonant tank on the load side. Taking all these points into consideration brings forth the desire to investigate the IGCT at low current switching conditions in order to gain knowledge and deeper understanding of the duration of switching transients, di/dt values, SOA conformity and switching energy losses in both hard switching and resonant circuit operation. The goal of this paper is to explore the quasi-soft switching of the IGCT under the typical LLC-SRC current and voltage stresses and characterize the turn-off process. Authors are not aware of any applications of the IGCT power switches in LLC-SRC or similar resonant topologies up to the moment of writing of this article.

LLC SRC Operation

Half-bridge LLC-SRC topology is presented on Fig. 1, with resonant circuit consisting of the resonant capacitor and the leakage inductance of the Medium Frequency Transformer (MFT). Design parameters for the given example (Fig. 1) are presented in the Table I and are based on the transformation ratio of

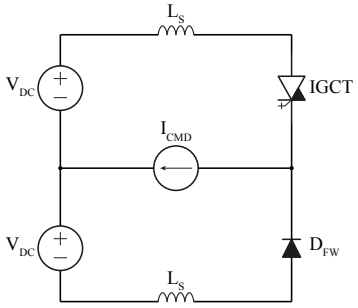

Fig. 4: Resonant operation diagram

Table II: Circuit parameters for resonant operation

Parameter	Value
V_{DC}	1250V
L_S	200nH
D_{FW}	Ideal diode
IGCT	5SLD 0600J65010
$I_{CMD}(0 \leq t \leq \frac{T_r}{2})$	$I_M \sin(2\pi f_r t) + 2 f_{SW} I_{OFF} t$
$I_{CMD}(\frac{T_r}{2} \leq t \leq \frac{T_{SW}}{2})$	$2 f_{SW} I_{OFF} t$
f_{SW}, f_r	1250Hz, 1389Hz

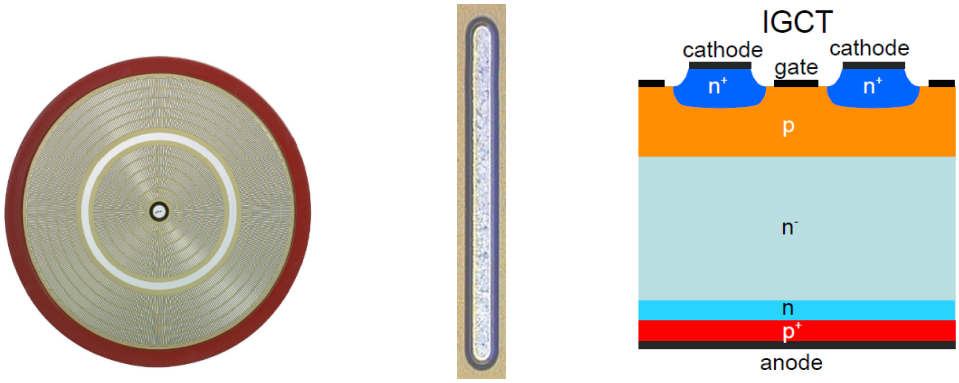

(a) (b) (c)

Fig. 5: a) GCT wafer, top view b) GCT finger, top view c) GCT simulation geometry, front view

2 with the rated power of 1.5MW. Typical waveforms for the primary side switches are shown in the Fig. 2. Half bridge configuration is selected because of its simplicity, employing the lowest amount of semiconductor switches for increased reliability of the converter. Medium frequency operation is desired for decreasing the size of the transformer which is a central part for voltage level transformation and electrical isolation between primary and secondary circuits. Resonant frequency is chosen to be slightly above the switching frequency. Fig. 3 shows the dependency of primary to secondary voltage ratio on a switching to resonant frequency ratio for various loads, starting from zero to full load. It can be noticed that for $0.8 \leq \frac{f_{SW}}{f_R} \leq 1.2$, output voltage is practically independent of the load; this flatness is the result of relatively high $\frac{L_M}{L_R}$ ratio, which is close to 30 in the given example. Switching frequency below the resonance allows for the turn-off current of the IGCT to be precisely defined and fixed in the design phase of the converter thus making the turn-off losses fixed and independent of load.

IGCT is chosen as switching element because of it robustness, very low conduction losses and high reliability. This paper provides more insight in the feasibility of integrating IGCT as a switching element in the LLC-SRC and shows the influence of the load current shape on the turn-off duration, energy losses and overall stability of the switch in the given operating conditions not typical for this kind of device.

IGCT turn-off current can be specifically controlled by tailoring the magnetizing inductance of the transformer. Decreasing the turn-off current has a positive impact on the turn-off energy losses which become significantly lower and accurately predictable since the turn-off current stays the same from one switching period to another. Low turn-off current has some undesirable effects on the operation that will be discussed further through the paper.

TCAD Simulations

TCAD model of the test IGCT was implemented in the Synopsis Sentaurus TCAD simulation package capable of accurate prediction of the semiconductor behaviour under different user specified loads. The

Table III: Resonant operation test circuit parameters

Parameter	Value
V_{DC}	$2x1250V$
C_{DC}	$2.6mF$
C_R	$657\mu F$
L_R	$15\mu H$
f_R	$1630Hz$
L_M	$1.5mH$, $3mH$, $6mH$
$IGCT_1, IGCT_2$	5SHX 1445H
D_1, D_2	5SDF 10H4503
L_σ	$800nH$

Table IV: Reverse conducting IGCT data

	IGCT	Reverse Diode
Manufacturer	ABB	ABB
Model	5SHX 1445H	5SHX 1445H
Forward		
blocking voltage	5500V	5500V
V_{DC}	3300V	-
I_{TGQM}	900A	-
I_{FAVM}	-	170A
Threshold Voltage	1.65V	2.53V
Slope Resistance	$2m\Omega$	$4.3m\Omega$

tool is based on the finite element method for solving the fundamental partial differential equations representing the silicon wafer in a semiconductor device e.g. transport and diffusion equations. One of the advantages of the package, interesting for this paper, is the ability for the user to define SPICE based description of the circuit around the TCAD modelled device in order to predict the behaviour of the given device under the specific circuit conditions. This fact is used for obtaining the first on/off waveforms of the IGCT under test and later compare the simulation data to the actual experiment.

IGCT is simulated with the circuit environment that corresponds to operation of the typical LLC-SRC (Fig. 4) with the parameters as described in the Table II, while the model of the semiconductor is simulated in the finite element manner. The difference between the actual test setup and the simulation is that the simulation's free-wheeling diode D_{FW} is implemented as the ideal diode.

Figures 5a-5c roughly show the steps in modelling of the semiconductor geometry. GCT wafer (Fig. 5a) consists of many GCT fingers (Fig. 5b) spread across the circular surface of the wafer. Modelling of all the fingers would be very time consuming and would not improve the accuracy of the model considerably; instead only one GCT finger is modelled and simulated in 2D with half the geometry and symmetrical boundary conditions along the edges (Fig. 5c). By using proper upscale coefficients, all the values of interest for the full GCT wafer are obtained.

Preliminary simulations show that there is no significant influence of the load current shape on the IGCT turn-off behaviour (Fig. 6 and Fig. 7; small artificial bias is added to the waveforms in Fig. 7 to avoid the overlapping) when compared to the typical double pulse test presented in [8]. Parameter I_M is used to set the maximum value of the resonant part of the current as defined in the Table II. This finding suggests that a typical double pulse data found in the datasheet of the device could be used in the design stage of the converter, given that it is available for the low values of the load current. However, it should be noted that the conduction time of the IGCT considered during the simulation is much longer than its recombination time constant so it is safe to assume that the shape of the conduction current of the IGCT has no influence on the stored charge; it depends only on the turn-off current value. Analysis performed in [9] for the IGBT suggests similar results.

It is observed that decrease of the turn-off current extends the time needed for the IGCT to successfully enter the blocking state i.e. lower the turn-off current, longer the turn-off delay time (t_{DOFF}) shown in the Fig. 9. t_{DOFF} should not change considerably during the steady state operation of the converter since the turn-off current is fixed and defined during the design process (there is a slight variation with temperature) but its knowledge and prediction is crucial on the choice of resonant frequency of the LLC-SRC and proper dead time definition.

Test Setup Measurements

Test setup given in Fig. 10 has been designed and implemented for the purposes of testing the IGCT switching devices under different working conditions (both hard-switching and resonant). Functionality

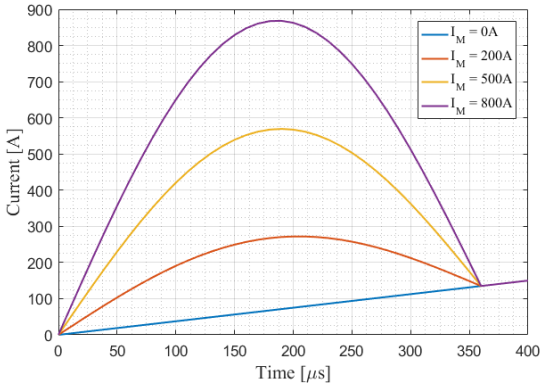

Fig. 6: Preflooding of the IGCT, $I_{OFF} = 150A$

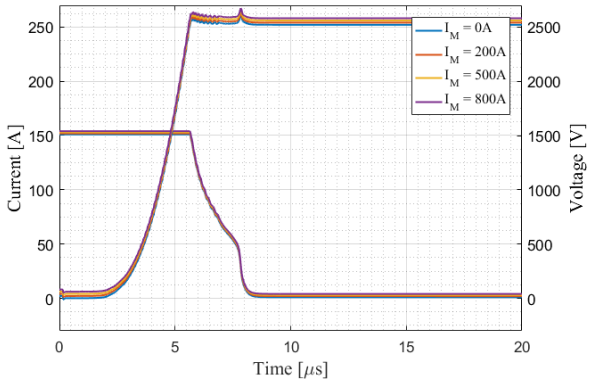

Fig. 7: IGCT turn-off UI waveforms, $I_{OFF} = 150A$

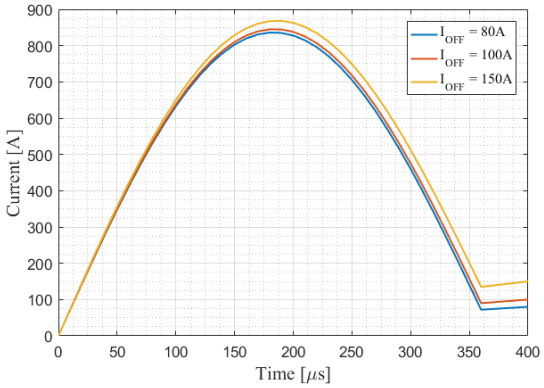

Fig. 8: Preflooding of the IGCT, $I_M = 800A$

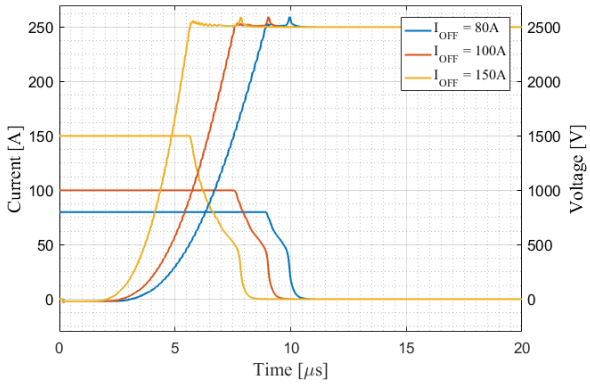

Fig. 9: IGCT turn-off UI waveforms, $I_M = 800A$

of interest for this paper is its ability to produce voltage and current stress on a device under test in a same manner as if the device was used in the LLC-SRC. The test will provide detailed practical insight of the device's turn-on and turn-off behaviour in te LLC-SRC topology, SOA conformity and switching energy losses. Electrical diagram of the circuit used for the resonant operation test is presented in the Fig. 11 (one out of four possible modes of use of test setup) and the actual circuit parameters are given in the Table III. This assembly allows for pulsed testing of the IGCT i.e. building up of only one pulse of the resonant current and its turn off as well as continuous operation of the switches for the longer heat run test. Detailed reverse conducting IGCT data is given in Table IV.

Resonant pulse test is performed by firstly charging the DC-link to the predefined level (2.5kV in this case) followed by charging of C_R and setting it to the value that corresponds to the desired peak of the resonant circuit current (i_{LR}). Turn-on pulse is later sent to the $IGCT_2$ (while $IGCT_1$ is kept off all of the time) which causes linear current build up in the L_M inductor as well as triggering the oscillation in the L_R - C_R circuit. The sum of these two electrical currents is passing through the $IGCT_2$ until it is commanded to turn-off i.e. after half of the switching frequency period. This way, the LLC-SRC turn-off condition is achieved for the device under test. It should be noted that this operation causes the $IGCT_2$ current to start from zero and not from the negative value (negative current is supported by the anti parallel diode integrated into the device) as found in LLC-SRC.

For fully emulating LLC-SRC turn-off condition, both switches must be manipulated and this is the second step in the resonant pulse testing. In order to achieve the same turn-off current as in the previous test, L_M must be decreased by half, while keeping the DC-link voltage the same. Test starts by pre-charging DC-link and C_R, as in previous step, but now $IGCT_1$ is turned on first for the duration of one quarter of the switching frequency period, followed by turning on the $IGCT_2$ for the next half of the switching period. This way, positive current is build up in the L_M and after turning the $IGCT_1$ off, this current is commutated to the free-wheeling diode of the $IGCT_2$ and resonant current is triggered in the L_R

Fig. 10: IGCT test setup

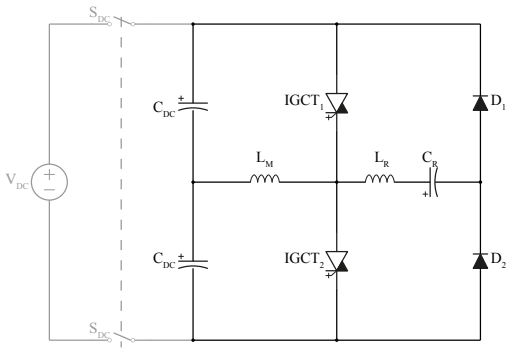

Fig. 11: Resonant operation equivalent circuit

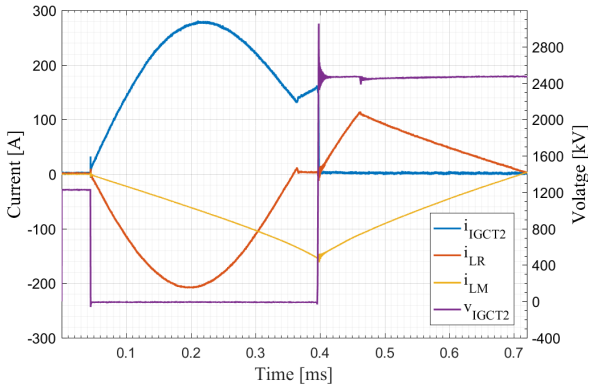

Fig. 12: One switch resonant pulse

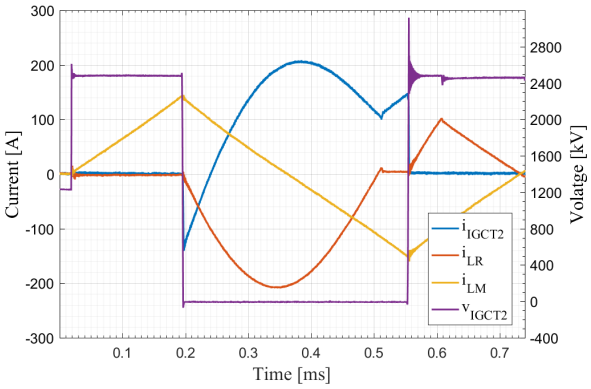

Fig. 13: Resonant pulse using both IGCTs

- C_R. After the required dead time, $IGCT_2$ is turned on and takes over the sum of i_{LR} and i_{LM}. It should be noted here that $IGCT_2$ must be pulsed before the moment when current in its free-wheeling diode reaches zero to ensure proper operation. Turn-on time window grows shorter as the resonant frequency is increased and must be taken into account in the design phase of the converter since the same effect is present there as well. Low current turn-off shows its influence on the choice of resonant frequency: if the t_{DOFF} of the $IGCT_1$ is too long, turning on the $IGCT_2$ could bring the DC-link to short circuit. Designer is now presented with a choice of lowering both resonant and switching frequencies (while keeping their ratio constant) or increase the turn-off current.

Experiments with constant turn-off current I_{OFF}

The first set of resonant pulse experiments (Case A) was performed by switching only $IGCT_2$ for a fixed amount of time, $350\mu s$ in this case, while keeping the DC-link voltage constant at 2.5kV. With fixed magnetizing inductor of 3 mH, turn-off current is held constant at 145.8 A, whereas the amplitude of the resonant current was varied by pre-charging the resonant capacitor to different voltage levels. Equation 1 shows the dependance between the resonant current peak - I_M and the resonant capacitor voltage before switching - U_{C0}, assuming known parameters of the resonant circuit (given in Table III for this experiment) and lossless components. Measured current waveforms are shown in the Fig. 14.

$$I_M = U_{C0}\sqrt{\frac{C_R}{L_R}} \tag{1}$$

Second set of experiments (Case B) was done by manipulating both $IGCT_1$ and $IGCT_2$ in order to achieve the zero voltage turn-on of the $IGCT_2$. DC-link voltage and the pulse duration are kept same as in the previous set of experiments but with the different magnetizing inductor of 1.5 mH in order to achieve the turn-off current of 145.8A. Resonant current peak variation was done in the same manner as in previous step and the results are presented in the Fig. 15.

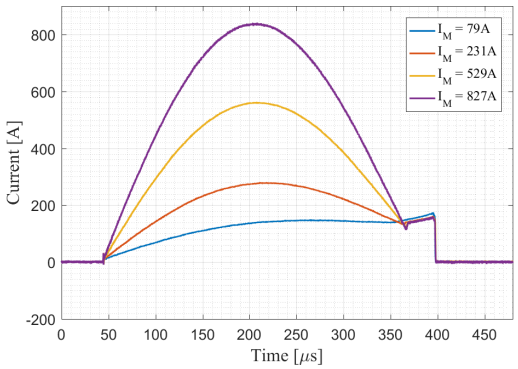

Fig. 14: $IGCT_2$ resonant pulse currents, Case A

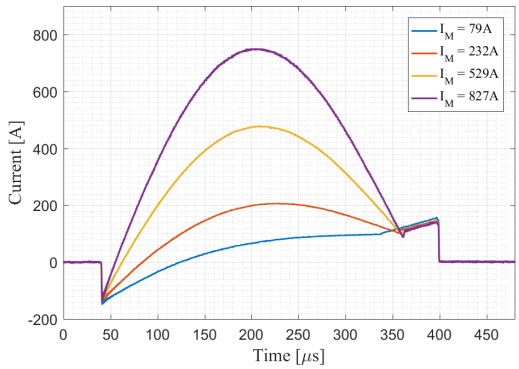

Fig. 15: $IGCT_2$ resonant pulse currents, Case B

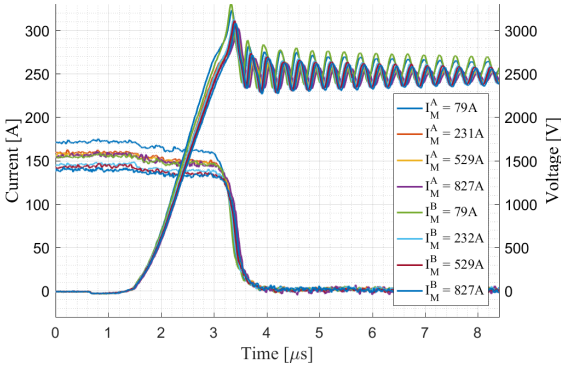

Fig. 16: Turn-off transient current and voltage waveforms, Cases A and B

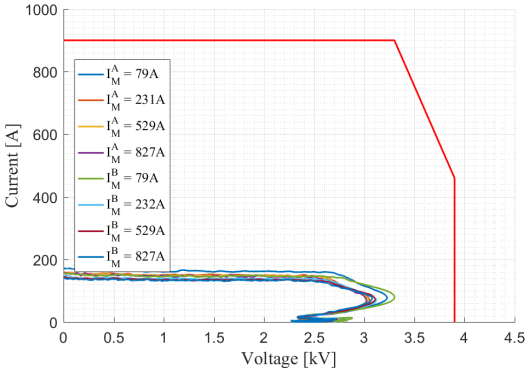

Fig. 17: Turn-off transient current and voltage SOA conformity, Cases A and B

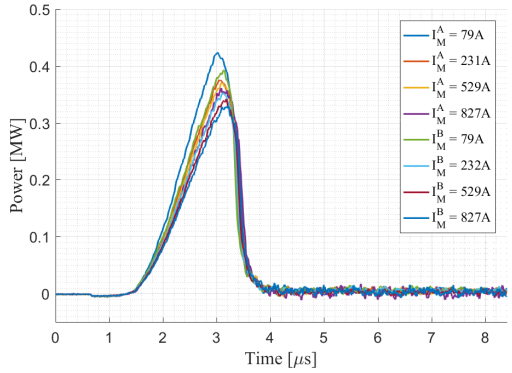

Fig. 18: Turn-off power losses, Cases A and B

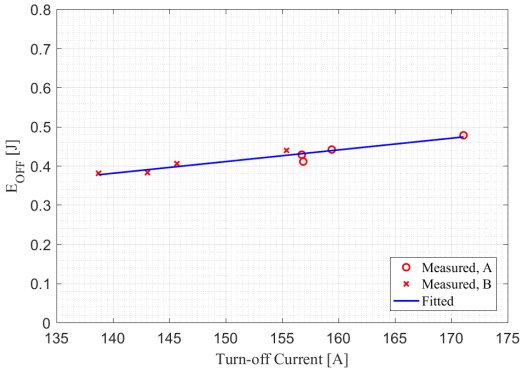

Fig. 19: Turn-off energy losses, Cases A and B

Fig. 16 presents the characteristic turn off transient waveforms of the IGCT under test i.e. $IGCT_2$. It can be noticed that there in no significant influence of the resonant current pulse amplitude on the turn-off waveforms in terms of turn-off delay time. Small deviation of the turn-off current values is due to deviation of the DC-link voltage from test to test. Significant ringing in the IGCT's anode to cathode voltage is explained by the presence of the relatively large parasitic inductance (800nH) in the commutation circuit. It should be noted that TCAD simulations were performed with the much lower parasitic inductance (200nH). Even with this parasitic value SOA is not violated, which is shown in Fig. 17. Power and energy losses of the switch under test are are presented in Fig. 18 and Fig. 19 respectively. It can be safe to state that under the given switch loadings, history of the conduction current does not significantly influence the turn-off energy losses and the t_{DOFF} of the IGCT.

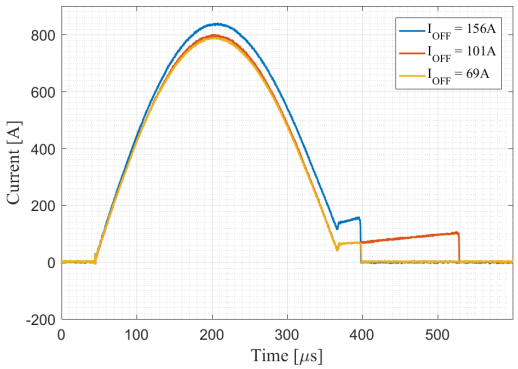

Fig. 20: $IGCT_2$ resonant pulse currents, Case A

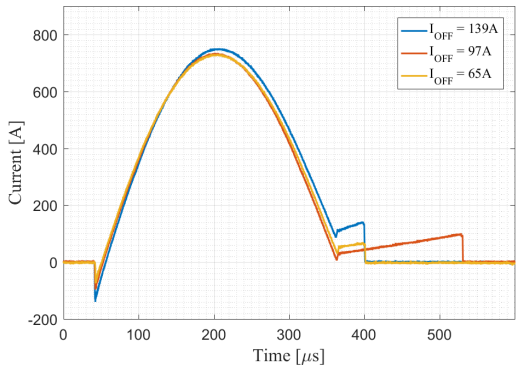

Fig. 21: $IGCT_2$ resonant pulse currents, Case B

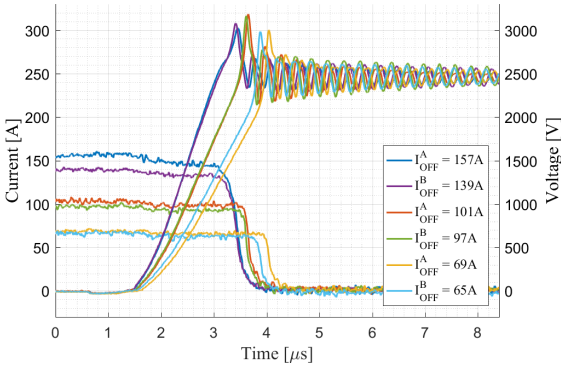

Fig. 22: Turn-off transient current and voltage waveforms, Cases A and B

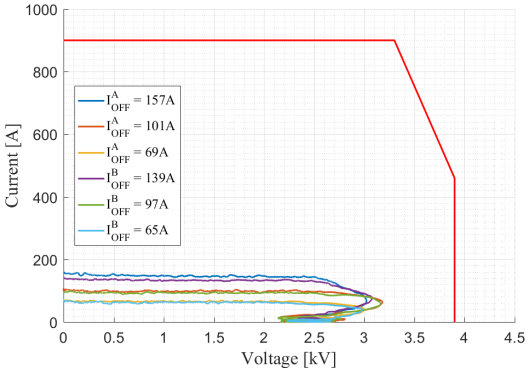

Fig. 23: Turn-off transient current and voltage SOA conformity, Cases A and B

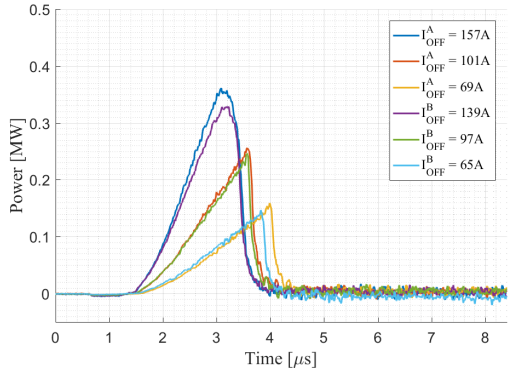

Fig. 24: Turn-off power losses, Cases A and B

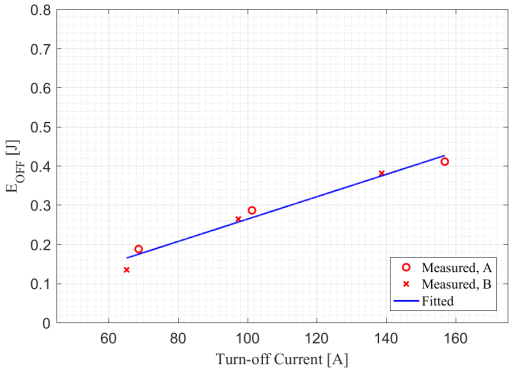

Fig. 25: Turn-off energy losses, Cases A and B

Experiments with constant resonant current amplitude I_M

Second part of the resonant pulse experimentation was performed in order to observe the IGCT turn-off behavior under the different turn off currents while keeping the resonant part constant. DC-link voltage was kept at 2.5kV with the pulse duration of 350μs and 480μs, depending on the desired turn-off current. Current waveforms of the $IGCT_2$ for the single switch manipulation set of results (Case A) are presented in Fig. 20 while Fig. 21 shows the waveforms under two switch operation (Case B), both for the three different turn-off currents. Detailed turn-off transition is shown in Fig. 22 presenting both cathode current and anode to cathode voltage of the $IGCT_2$. Influence of the turn-off current value on the turn-off delay time is clearly visible and suggests the same behavior as in the hard switched applications of the IGCT. Ringing in the voltage, caused by relatively high parasitic inductance, is evident but the SOA is not violated (Fig. 23). Power and energy losses graphs (Fig. 24 and Fig. 25) show the strong influence

of the turn-off current on its values and comparison with the results from [8] (with the same device under test) yields a conclusion that the turn-of behavior remains the same irrespective of the mode of operation (hard switched or resonant operation). Again, pulse duration is much longer that the recombination time constant.

Conclusion

Prospect of low overall energy losses of the IGCT opens the opportunity of increasing its switching frequency allowing for the decrease in volume of the surrounding passive components of the LLC-SRC. Preliminary simulation results indicate that resonant pulse present during the conduction phase of the IGCT does not affect the turn-off process making the use of datasheet values (e.g. $E_{OFF}(I_{OFF})$), provided for hard switching conditions, justified in the design stage of the converter. It is already shown that low turn-off currents prolong the duration of turn-off process [8] which is in conflict with the desire of increasing the switching frequency so the designer must find an optimum compromise between the switching frequency and turn-off energy losses.

Experimental results presented in this paper confirm the TCAD simulation outcomes that the shape of the conduction current of the IGCT does not influence its turn-off behavior in terms of energy losses and turn-off delay times. Deciding factor for the selected parameters is the turn-off current which allows for the datasheet or hard-switched operation values (E_{OFF}, t_{DOFF}) to be used during the design process of the LLC-SRC.

References

[1] D. Dujic, F. Kieferndorf, F. Canales, and U. Drofenik. “Power electronic traction transformer technology”. In: *Power Electronics and Motion Control Conference (IPEMC), 2012 7th International*. Vol. 1. IEEE. 2012, pp. 636–642.

[2] S. Kenzelmann, A. Rufer, D. Dujic, F. Canales, and Y. R. De Novaes. “Isolated DC/DC structure based on modular multilevel converter”. In: *IEEE Transactions on Power Electronics* 30.1 (2015), pp. 89–98.

[3] P. K. Steimer, H. Gruning, J. Werninger, E. Carroll, S. Klaka, and S. Linder. “IGCT - a new emerging technology for high power, low cost inverters”. In: *IEEE Industry Applications Magazine* 5.4 (1999), pp. 12–18.

[4] Y. Suh and P. K. Steimer. “Application of IGCT in high-power rectifiers”. In: *IEEE Transactions on Industry Applications* 45.5 (2009), pp. 1628–1636.

[5] W. Raithmayr, P. Daehler, M. Eichler, G. Lochner, E. John, and K. Chan. “Customer Reliability Improvement with a DVR or a DUPS”. In: *Power World* 98 (1998), pp. 1–10.

[6] U. Vemulapati, M. Rahimo, M. Arnold, T. Wikström, J. Vobecky, B. Backlund, and T. Stiasny. “Recent advancements in IGCT technologies for high power electronics applications”. In: *Power Electronics and Applications (EPE’15 ECCE-Europe), 2015 17th European Conference on*. IEEE. 2015, pp. 1–10.

[7] D. Dujic, S. Lewdeni-Schmid, A. Mester, C. Zhao, M. Weiss, J. Steinke, M. Pellerin, and T. Chaudhuri. “Experimental characterization of LLC resonant DC/DC converter for medium voltage applications”. In: *Proceedings of the PCIM Europe 2011*. 2011, pp. 265–271.

[8] D. Stamenkovic, U. R. Vemulapati, M. Rahimo, T. Stiasny, and D. Dujic. “IGCT Switching Behaviour Under Low Current Conditions”. In: *Proceedings of the PCIM Europe 2018*. 2018, pp. 777–782.

[9] G. Ortiz, H. Uemura, D. Bortis, J. W. Kolar, and O. Apeldoorn. “Modeling of Soft-Switching Losses of IGBTs in High-Power High-Efficiency Dual-Active-Bridge DC/DC Converters”. In: *IEEE Transactions on electron devices* 60.2 (2013), pp. 587–597.